

FIRST RESULTS OF REGRESSION RATE MEASUREMENTS ON ULTRASONIC BASIS  
IN THE AHRES HYBRID ROCKET MOTOR

**Dennis Pormann**

German Aerospace Center (DLR), Institute of Aerodynamics and Flow Technology, Germany, dennis.pormann@dlr.de

J. Wilken\*, O. Božić<sup>†</sup>, D. Lancelle<sup>‡</sup>

German Aerospace Center (DLR), Institute of Aerodynamics and Flow Technology, Germany

ABSTRACT

**For the experimental investigation of the regression-rate characteristics of a hybrid rocket motor an ultrasonic measurement system was built up. As solid fuel hydroxyl-terminated polybutadiene (HTPB) with aluminium particles is used and 87.5% hydrogen peroxide as oxidizer. The instantaneous solid-fuel regression rate was measured at 2 points in axial location during one 10 s firing test. Several physical properties of the fuel were determined in order to correct the ultrasonic pulse flight time from errors due to the heat profile and chamber pressure. Results of the "Lumped Pressure Correction Method" are presented and an extension to this method is shown.**

NOMENCLATURE

c	sound velocity
p	pressure
T	Temperature
t	time
w	web thickness
$\varepsilon_a$	artificial strain [6]
$\tau$	propagation time of ultrasound signal

Subscripts

p	propellant
ref	reference condition (0.1 MPa)
mean	averaged data
dynamic	unsteady component
corr	corrected

I. INTRODUCTION

Hybrid rocket engines are known for over 80 years and are still not in use for launcher systems. They comprise advantages like low price production, inherent safety, ecologically friendliness and throttle ability among others. A primary problem in hybrid rocket propulsion is the regression rate of the solid fuel. It depends on the flow features inside the combustion chamber and is therefore different for each propellant combination and changes with engine size and also with burn time.

\*German Aerospace Center (DLR), Institute of Aerodynamics and Flow Technology, Germany, jascha.wilken@dlr.de

<sup>†</sup> German Aerospace Center (DLR), Institute of Aerodynamics and Flow Technology, Germany, ognjan.bozic@dlr.de

<sup>‡</sup> German Aerospace Center (DLR), Institute of Aerodynamics and Flow Technology, Germany, daniel.lancelle@dlr.de

The DLR investigates the mechanisms which affect the regression rate within the project AHRES [1] (Advanced Hybrid Rocket Engine Simulation). A database with experimental firing tests is going to be established. Real time regression rate data are needed to investigate the mechanisms which influence the solid fuel regression.

Two non-intrusive principles are known for this purpose, X-ray radiography and ultrasonic measurement. The first technology is difficult to conduct on rocket engines which comprise a 3D grain geometry, because the 2D images gained will be influenced by objects that lay in front or behind the surface to be measured. But it is a good choice for 2D slab burner, because data is gained for the whole grain and not just for certain points.

Ultrasonic measurement is done on solid and hybrid rocket engines since 1965. A summary of different investigations is given in [2]. The basis is to measure the time an ultrasonic signal needs to travel through the fuel grain. If the sonic velocity of the fuel grain is known it is a direct measure for the thickness. Unfortunately, the sonic velocity is influenced by the chamber pressure and temperature profile inside the grain.

Here the ultrasonic principle is used for regression rate determination, because it is applicable on powerful operational engines.

II. EXPERIMENTAL METHOD

II.1 Hybrid Rocket Engine

The hybrid rocket engine geometry is shown in Figure (1). As oxidizer hydrogen peroxide ( $H_2O_2$ ) with a concentration of 87.5% is applied. A catalyst chamber is used to decompose the hydrogen peroxide into hot steam and oxygen at a temperature of approx. 650°C. The catalyst itself consists of pure silver meshes. In front of the catalyst bed an injector head is used to spread the  $H_2O_2$  equally inside the chamber and to prevent instabilities caused by pressure fluctuations. Due to the catalyst chamber no other ignition system is needed.

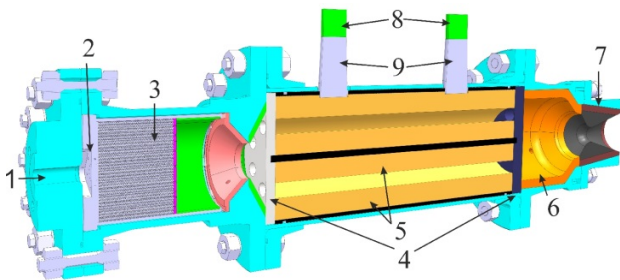


**Fig. 1: AHRES Hybrid rocket engine: 1 oxidizer inlet; 2 injector head; 3 silver mesh; 4 vortex plates; 5 fuel; 6 heat shield; 7 graphite nozzle; 8 ultrasonic transducer; 9 delay line**

The fuel grain geometry is a telescope configuration, thus an inner cylinder and an outer cylinder are arranged concentrically. Overall length of the grain is 376 mm. Inner cylinder diameter is 55 mm and outer cylinder diameter is 90 mm on the inside, and 140 mm on the outside. Thus, the web thickness is 25 mm. Of course, the regression measurement can only be done on the outer cylinder. Advantages of the telescope configuration are a high load factor and a low oxidizer/fuel-shift (O/F) over time, because the surface change is small. The fuel consists of hydroxyl-terminated polybutadiene (HTPB) mixed with aluminium powder.

A vortex plate at the entrance to the combustion chamber is used to retain the inner cylinder and to study the influence region downstream the vortex plate. To prevent chemical effects of the oxidizer with the vortex plate, it is made of aluminium oxide. The second vortex plate downstream the fuel grain serves as the second retainer for the inner fuel grain and induces turbulence inside the vortex chamber to enable a good energy efficiency due to complete chemical reaction. This plate consists of carbon-fibre/phenolic like the heat shield, which prevents damage to the inconel engine hull. The conical nozzle is made of isostatically pressed graphite and is adapted to ambient pressure.

Some special properties of this engine should be emphasized. Because the oxidizer is completely decomposed, droplet atomisation and impinging of droplets on fuel surface do not occur. Furthermore, the oxidizer is hot when it enters the combustion chamber and therefore it has a comparatively high speed at the leading edge.

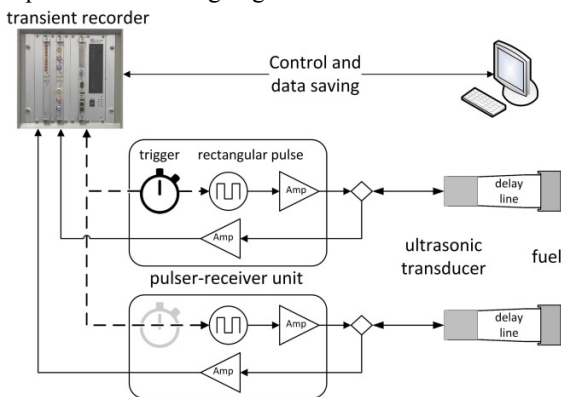


**Figure 2: Ultrasonic setup**

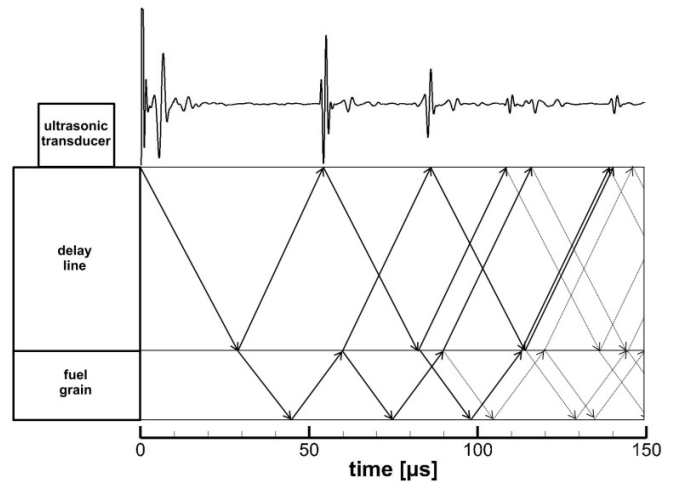


**Figure 3: Ultrasonic signal with refraction paths**

## II. II Ultrasonic Hardware Setup

The hybrid rocket engine is equipped with 2 ultrasonic transducers which have an active area diameter of 25 mm and 1 MHz nominal frequency. They are mounted 20.74% and 71.59% of grain length downstream of the catalyst chamber.

In order to protect the ultrasonic transducers from stress due to chamber pressure and heat from the combustion gases a delay line is used. Its material has to be suitable to the solid fuel acoustic properties enabling a large amount of ultrasonic energy to travel into the fuel. The length of the delay line has to be chosen that no overlay with other echos can appear during the measurement time. The planar surface for the delay line on the solid fuel was made during casting of the grain. For a better coupling a gel based on silicone was coated on this surface.

The ultrasonic pulse, with a length of 1  $\mu$ s and an amplitude of 400 V, is generated by a square wave pulser-receiver unit for each transducer. The mechanical pulse, reflected at the border between solid fuel and combustion gases, is converted into an electrical signal by the ultrasonic transducer which is then amplified by the receiver section. The resulting radio frequency is digitized by an Amotronics transient recorder (Fig. 2).

This transient recorder is able to digitize the return signal at 100 MHz and 14 bit resolution. The return signal is stored for the whole roundtrip time of the ultrasonic pulse, plus some extra time to see the reflections of the main signal. Overall 150  $\mu$ s were stored for each ultrasonic pulse (Fig. 3). Due to the high data rate the transient recorder has to store the data in the system RAM. Therefore about 4000 samples can be stored for each measurement point. To store the whole test run data of the 10 s firing test and a part of the engine cool down phase, the measurement was carried out at 100 Hz ultrasonic pulse repetition rate.

### II.III Properties of the fuel

The fuel consist of 70%wt HTPB and 30%wt aluminium particles, with a mean diameter of 5  $\mu\text{m}$ . For ultrasonic speed calibration and the determination of other fuel properties a calibration body is casted for every fuel grain. It involves 4 different heights for the calibration, namely 20 mm, 40 mm, 50 mm and 100 mm (Fig. 4). For an ultrasonic regression measurement the speed of sound, depending on temperature and pressure, needs to be known. At reference conditions the speed of sound in the fuel is 1470 m/s. In particular the influence of temperature effects on the speed of sound were examined by heating and cooling the calibration body to specific temperatures and subsequent measurement of the resulting speed of sound. Of course, also the thermal expansion of the calibration body has to be considered during this experiment. Higher temperatures led to a lower speed of sound. The effect of temperature was only examined up to 375 K, where the speed of sound falls to 1140 m/s.

The thermal expansion of the calibration body was also measured and it was found that the errors introduced by thermal expansion are only a fraction of the errors introduced by the changing speed of sound.

The temperature of the fuel grain also influences the sound attenuation coefficient. Higher temperatures result in lower attenuation coefficients and thus in better ultrasonic echoes. The aluminium particles should not have an effect on attenuation, because they are much smaller than the wavelength at 1 MHz (1.5 mm). However, the attenuation coefficient was higher with aluminium particles than for pure HTPB in this calibration body.

In order to correct for temperature effects it is not sufficient to know the speed of sound at relevant temperatures, but additional information regarding the development of the thermal boundary layer is needed. To attain this information a numerical model of the fuel grain, based on the model discussed in [3], was developed. Input parameters for the model are thermal conductivity, thermal capacity and density.

The density was determined by comparing the weight of the calibration body with its volume resulting in a density of 1140  $\text{kg}/\text{m}^3$ .

Thermal capacity was simply calculated as the weighted average of the thermal capacity of the fuel components. Thus, the fuel sample of 70%wt HTPB (1632.8  $\text{J}/\text{kg}\cdot\text{K}$  [4]) and 30%wt aluminium (897  $\text{J}/\text{kg}\cdot\text{K}$ ) has a thermal capacity of 1412.06  $\text{J}/\text{kg}\cdot\text{K}$ .

For the determination of the thermal conductivity coefficient a fuel sample with a thickness of 20 mm was placed on a hot aluminium cuboid, with a temperature of 160  $^{\circ}\text{C}$ . The surface temperature on the outer side of the fuel sample was measured and compared to results of the numerical simulation. A parameter study showed that a thermal conductivity coefficient of 0.3  $\text{W}/(\text{m}\cdot\text{K})$  fits the experimental results best. Hence, it can be stated that aluminium particles have just a small influence on the thermal conductivity compared to pure HTPB (0.26  $\text{W}/(\text{m}\cdot\text{K})$ ).

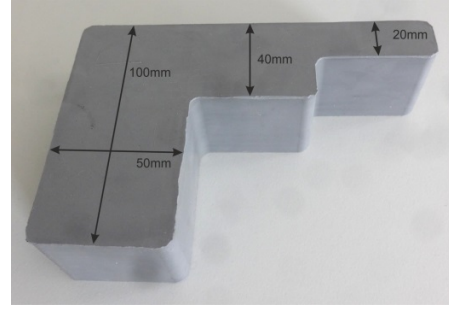


**Figure 4: Calibration body**

### II.IV Signal Detection

Data analysis was done in post processing only, hence no real time regression rate data was available. The automatic detection of the roundtrip time was done by cross correlation, which was done with a manually extracted echo signal as pattern [5]. Although the amplitude of the echo signal changes during the test run, the position is always detected reliably.

Since the fuel has a sonic velocity of approximately 1500 m/s and the return signal is sampled at 100 MHz, the spatial resolution is 15  $\mu\text{m}$ . As the fuel grain is passed 2 times, the resolution of the thickness is 7.5  $\mu\text{m}$ . For the calculation of the regression rate the central difference quotient (Eq. 1A) is used. Therefore, the resolution of the regression rate is 0.375  $\text{mm}/\text{s}$  (Eq. 1B). Of course, if the time interval is set longer than 0.02 s, the resolution of the regression rate will be better, which is identical with a smoothing of the data. If a high resolution for the regression rate is needed for a short time interval, the ultrasonic sample rate of 100 MHz has to be increased.

To raise the resolution at 100 Hz a parabolic approximation of the cross-correlation was done. At the peak of the correlation result the neighbourhood is fitted to a parabola. The time with highest correlation was set to the maximum of the parabola [5]. Figure (5) shows the result of this approximation.

$$\dot{f} = \frac{f(x+h) - f(x-h)}{2h} \quad (1A)$$

$$\dot{f} = \frac{7.5 \cdot 10^{-3} \text{ mm}}{2 \cdot 0.01 \text{ s}} = 0.375 \frac{\text{mm}}{\text{s}} \quad (1B)$$

### II.V Pressure Correction

The fluctuating pressure conditions in the rocket engine affect the ultrasonic measurement by two different mechanisms. In the first place the pressure compresses the fuel leading to a change in height and therefore an artificial regression of the fuel is measured by the ultrasonic system. Another error is introduced by the stress the pressure causes inside the fuel, it raises the speed of sound and thus a lower runtime of the ultrasonic signal is measured. From the perspective of the ultrasonic measurement this leads to a further compression of the fuel. In [6] the author developed

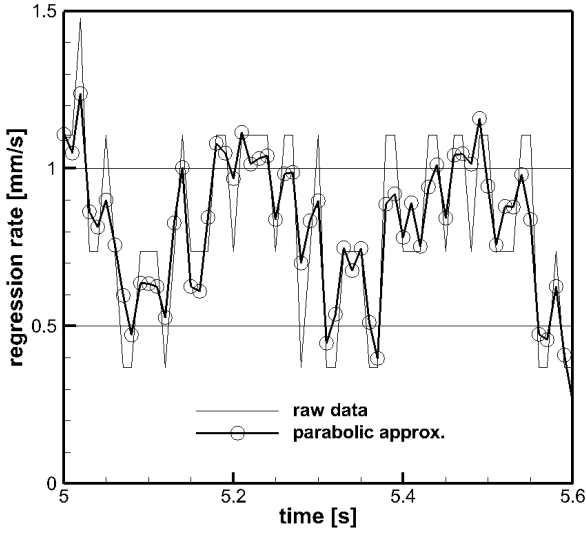


Fig. 5: Regression rate raw data vs. parabolic approx.

the “Lumped Pressure Correction Method” in order to correct these errors. This method is a simple approach where no material constants like bulks modulus, Young’s modulus and Poisson’s ratio are needed. The basic idea is to correct the time of flight without the need to know where the error comes from (Eq. 2).

$$\tau_{p,corr} = \tau_p + \left( \frac{\Delta \tau_p}{\tau_{p,ref}} \right) \tau_{p,ref} \quad (2)$$

The time of flight under atmospheric pressure  $\tau_{p,ref}$  is used to correct the difference  $\Delta \tau_p$  between reference condition and under pressure  $\tau_p$ . For this purpose the factor  $\varepsilon_a$ , artificial strain, is introduced that expresses the error caused by pressure effects (Eq. 3). This substitution leads to Equation (4).

$$\varepsilon_a(p) = \frac{\Delta \tau_p}{\tau_{p,ref}} \quad (3)$$

$$\tau_{p,corr} = \tau_p + \varepsilon_a(p) \cdot \tau_{p,ref} \quad (4)$$

The value of the factor  $\varepsilon_a$  depends on the pressure in the combustion chamber. If the value of  $\varepsilon_a$  is known for the range of pressures encountered in the combustion chamber, the measurement runtime can be corrected using the measured pressure in the chamber.  $\varepsilon_a$  is determined by a series of ultrasonic measurements at various pressures with neutral gas, conducted before the test run. The curve used for the correction of the burn test data is shown in Figure (6). As  $\varepsilon_a$  is a factor it can correct any thickness of the same material. For the correction,  $\tau_{p,corr}$  and  $\tau_{p,ref}$  in Equation (4) are supposed to be the same. In practice there can be small differences.

A further pressure driven effect is noted in [6]: The dp/dt-effect. Large dp/dt values lead to transient effects inside the grain, which in turn leads to errors in the ultrasonic pulse flight time. This effect seems to be connected to the momentary dp/dt value as well as the actual pressure value.

For tests with constant pressure levels the dp/dt effect only causes errors during the initial pressure buildup. If the pressure varies quickly during the test, the errors caused by this effect lead to large distortions of the measured regression rate.

In order to correct this error a variant of the “Lumped Pressure Correction Method” was developed. The pressure data was divided into two components: A semi-steady component,  $p_{mean}$ , which is the time averaged pressure curve, and an unsteady component  $p_{dynamic}$  that consists of the difference between the mean pressure and the current pressure. The semi-steady component is corrected according to the “Lumped Pressure Correction Method”. In addition the unsteady component is also subjected to this method, but the factor  $\varepsilon_a$  is amplified based on the semi-steady pressure level. Both correction factors are determined from the same curve, shown in Figure (6), but each factor is for another pressure value and the factor for  $\varepsilon_{a,dynamic}$  is additionally augmented, as shown in Equation (6).

$$\varepsilon_{a,mean} = \varepsilon_a(p_{mean}) \quad (5)$$

$$\varepsilon_{a,dynamic} = \varepsilon_a(p_{dynamic}) \cdot \frac{p_{mean}}{1 \text{ MPa}} \quad (6)$$

Equation (7) is the implemented form for the correction of the measured ultrasonic flight time.

$$\tau_{p,corr} = \frac{\tau_p}{(1 - \varepsilon_{a,mean}) \cdot (1 - \varepsilon_{a,dynamic})} \quad (7)$$

## II.VI Thermal Boundary Layer

Based on the aforementioned fuel properties and the numerical model, the thermal boundary layer was simulated. The temperature at the exposed edge of the fuel grain after ignition is assumed to be 1060 K based on the experiments performed in [7]. It was assumed, that the speed of sound

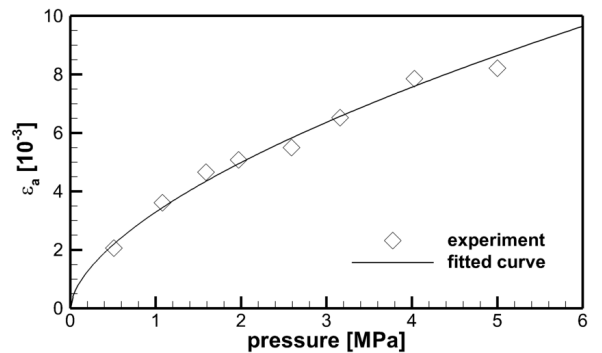
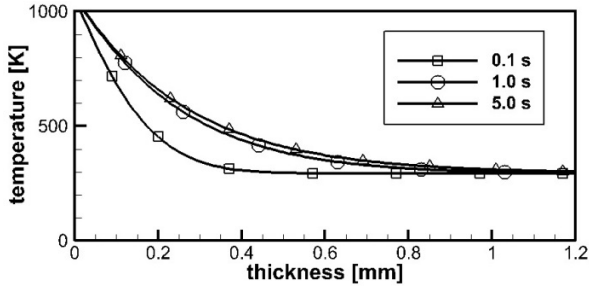


Figure 6: Artificial strain


**Figure 7: Temperature profile build up inside fuel grain**

continues to decrease linearly after 350 K since the breakdown products of HTPB have lower speed of sound than the original material [8]. Thus the data from the experiment were extrapolated to 600 K. The areas of the fuel grain that have temperatures above 600 K, the first 0.3 mm of the boundary layer, are not included in the correction since the manifold chemical reactions pose significant difficulties in ascertaining the local speed of sound of the fuel.

The results based on these assumptions show a constant thermal boundary layer with a final thickness of 2 mm, which corresponds to the results achieved by using the analytical equations described in [9]. Figure (7) shows the first 1.2 mm of the thermal boundary layer, where most of the changes happen during formation. However it takes time for the thermal boundary layer to achieve its final state. After two seconds 94% are reached and after five seconds the final state is established. While a constant thermal boundary layer only affects the calculation of the web thickness and not the regression rate, its transient formation has a noticeable effect on the regression rate measurement and thus should be corrected.

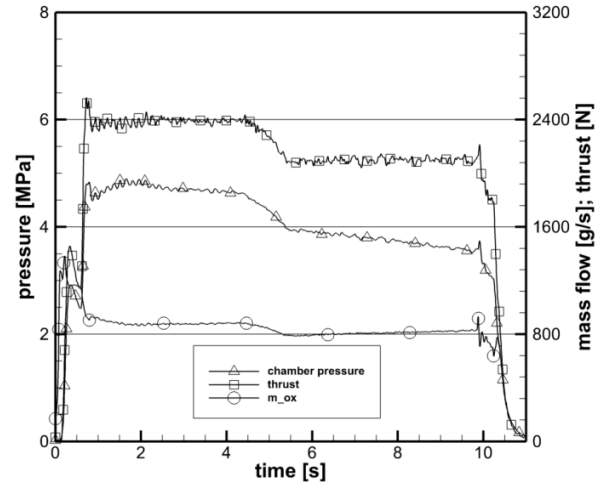
The correction implemented uses the numerical model to calculate the local temperature and speed of sound at any given time and location. The local speed of sound is calculated from the local temperature based on the experiments described in ‘‘Properties of the fuel’’. Using these data points a linear function was devised to approximate them. While evaluating these results the speed of sound at each temperature was calculated using the reference thickness of the calibration, not the actual thickness altered by thermal expansion as shown in Equation (8).

$$c_{corr}(T) = 2 \frac{w_{ref}}{\tau(T)} \quad (8)$$

This results in an artificial speed of sound, which when multiplied with the propagation time delivers a thickness comparable to the reference thickness and not skewed by thermal expansion. Later on the speed of sound is averaged using a harmonic mean as shown in Equation (9).

$$c_{mean,corr} = \frac{n}{\sum_{i=1}^n \frac{1}{c_i}} \quad (9)$$

Finally for each time step of the ultrasonic measurement all these factors are combined in Equation (10) with the  $\tau_{p,corr}$


**Figure 8: Hot test run data**

from Equation (7) to calculate the final corrected web thickness.

$$w_{corr}(t) = \frac{c_{mean,corr} \tau_{p,corr}(t)}{2} \quad (10)$$

### III. RESULTS

The hot test run was conducted at the DLR test facility in Trauen, Germany on the AHRES testbed. Overall test time was 10 s. The mean oxidizer mass flux was about 210 kg/m<sup>2</sup>·s which corresponds to a mean mass flow of 0.85 kg/s. As shown in Figure (8), the mass flow was throttled after 5 s for about 10%. At engine start the first pressure build up, at about 0.2 s, is generated by the oxidizer only. The second pressure rise starts at 0.6 s when the engine ignites. So, about 0.4 s were needed to heat up and gasify the solid fuel. At the time of ignition the temperature, of the decomposition products, was at 300°C. The static decomposition temperature of 650°C was reached after 3.5 s firing. The falling chamber pressure starting at 5 s is a consequence of nozzle erosion.

Figure (9) shows the raw data of the ultrasonic measurement. The thickness is calculated assuming a constant sonic velocity of 1470 m/s and the regression rate is calculated according Equation (1A).

The pressure build up phase at 0.2 s and 0.6 s causes a compression of the fuel grain, beside velocity changes due to stress, which is seen as a thickness decrease and therefore a high regression rate. As the chamber was pressurized the first time a part of the thickness change could also be caused by the settling phenomena of the delay line in the mount as well as changes in thickness of the gel between delay line and solid fuel.

Between second 1 and 3 chamber pressure fluctuations in the order of  $\pm 0.05$  MPa at about 7 Hz were observed. These oscillations can be caused by the catalyst chamber, because it has not reached its final temperature. The influence on the regression rate is clearly seen and should be corrected (Fig. 9).

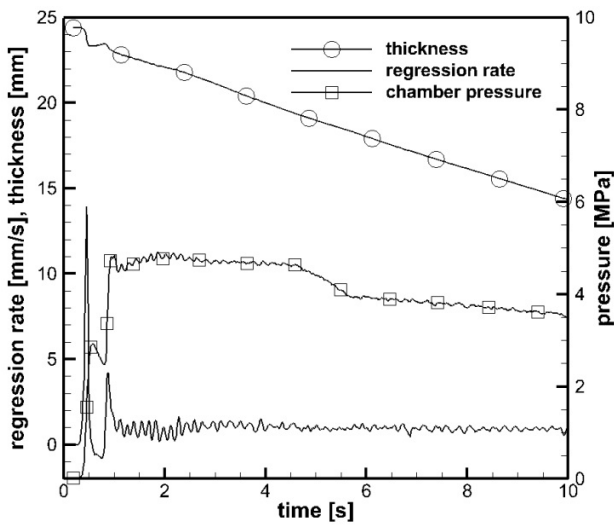


Figure 9: Ultrasonic data without correction

Figure (10) shows the regression rate in detail. The Lumped Pressure Correction Method only slightly effects the regression rate oscillations due to pressure. In contrast the extension to this method, developed in this study, can correct the pressure driven error up to 0.5 mm/s with an average correction of 0.14 mm/s within the range 1-3 s (Fig. 11). After 5 s firing time the pressure corrections are quite small with an average of 0.03 mm/s, because no prevailing pressure oscillations are present. The remaining oscillations in this region have to have another origin which is supposed to be a combustion effect.

Due to the vortex plate at the entrance of the fuel port the flow field on the fuel surface is different for both ultrasonic measurement points. Also the preeminent regression frequencies are different with 4.5 Hz near the catalyst and

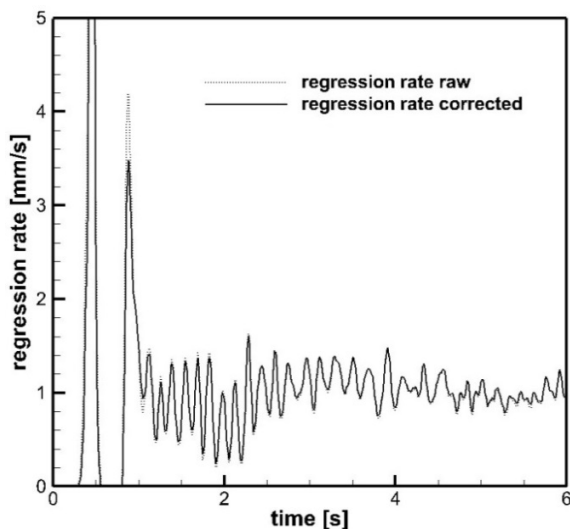


Fig. 10: Regression rate corrected by the Lumped Pressure Correction Method in original form.

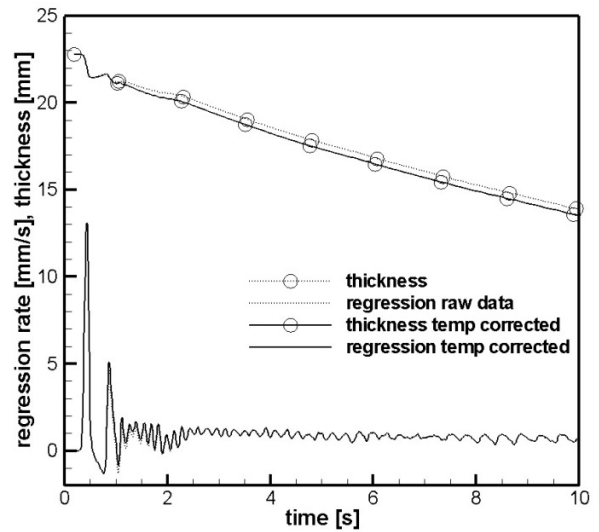


Figure 12: Temperature correction

2.7 Hz near the nozzle (compare Fig. 9, 12). The different frequencies exclude a pressure driven effect.

As expected, the fully developed temperature profile has no effect on the regression rate but causes a constant increase in thickness of 0.35 mm (Fig. 12). At engine start the temperature profile is still developing. Subsequently there is an influence on regression rate with a maximum error of 0.5 mm/s at engine start.

#### IV. CONCLUSION

The first operation of an ultrasonic measurement system in a hot firing test with the AHRES hybrid rocket motor was successful.

The “Lumped Pressure Correction Method” is not able to correct errors due to transient pressures but is applicable at

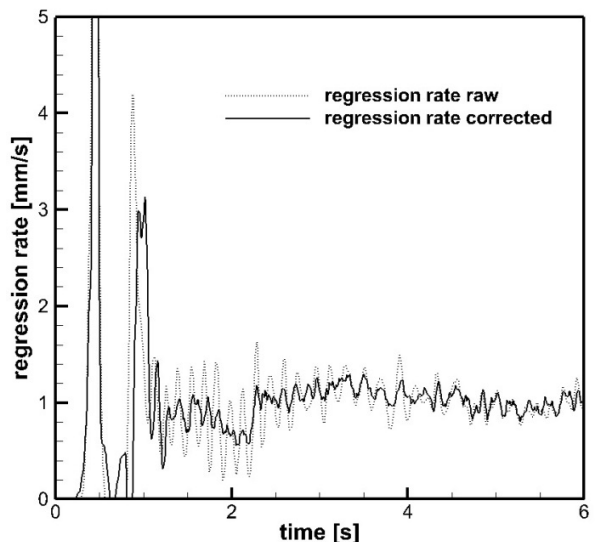


Fig. 11: Regression rate corrected by the introduced Lumped Pressure Correction Method extension.

static pressure conditions. An extension was introduced which can boost the correction in transient regions based on the mean pressure. The result looks plausible, but has to be tested in further firings. A lack of this method is the assumption, that the stress distribution inside the solid fuel grain will not change with time. This may be true for a 2D slab burner, but it is not for a 3D geometry.

Furthermore the temperature profile has no effect on the regression rate when it is fully developed. Only at engine start this effect has to be corrected. Due to the unknown sonic velocity above 600 K the results shown here are not completely temperature compensated.

Due to the applied correction an instability was found which could be caused by a combustion mechanism. This effect will be topic in future investigations.

#### V. ACKNOWLEDGEMENT

The authors kindly thank Mr. Wolfgang Kircher of company Sonotec who provided valuable comments and ideas regarding ultrasonic measurements. We also thank Mr. Martin Hessing of company Amotronics for the compilation of the ultrasonic measurement system. For support during the hot firing test our thanks goes to Noushin Mokhtari, Tobias Klaus, Stefan May, Georg Poppe and the staff of DLR Trauen.

#### REFERENCES

- 1 BOŽIĆ, O., PORRMANN, D., LANCELLE, D. AND HARTWIG, A., "*Program AHRES and its Contribution to Assess Features and Current Limitations of Hybrid Rocket Propulsion*", IAC-12-C4.2.8, October 2012, Naples, Italy
- 2 CAUTY, F., CARMICINO, C., "*The Pressure Sensitivity of the Ultrasonic Waves Velocity: A Contribution to a Better Determination of the Energetic Material Regression Rate.*", International Journal of Energetic Materials and Chemical Propulsion 6.6 (2007).
- 3 LANCELLE, D.M., BOŽIĆ, O. "*Simulation of an Ablative Thermal Protection System for Hypersonic Ascend of an Electromagnetically Launched Payload Carrier*", 5<sup>th</sup> European Conference for Aeronautics and Space Sciences (EUCASS), München, 2013
- 4 LENGELLE, G. "*Solid-Fuel Pyrolysis Phenomena and Regression Rate, Part I: Mechanisms.*", Progress in Astronautics and Aeronautics 218 (2007): 127.
- 5 MURPHY, J., KRIER, H. "*Evaluation of Ultrasound Technique for Solid-Propellant Burning-Rate Response Measurements*", Journal of Propulsion and Power, Vol.18, No.3, May-June 2002
- 6 SERIN, N., CHIAVERINI, M.J. "*Pressure Correction of Ultrasonic Regression Rate Measurements of a Hybrid Slab Motor*", AIAA Joint Propulsion Conference and Exhibit, Los Angeles, 1999
- 7 CHIAVERINI, M. J. ET AL., "*Regression-Rate and Heat-Transfer Correlations for Hybrid Combustion*", Journal of Propulsion and Power, 17.1 (2001): 99-110.
- 8 CHIAVERINI, M. J. ET AL., "*Pyrolysis behavior of hybrid-rocket solid fuels under rapid heating conditions*", Journal of Propulsion and Power 15.6 (1999): 888-895
- 9 MARXMAN, G.A., WOOLRIDGE, C.E., MUZZY, R.J. "*Fundamentals of hybrid boundary layer combustion*" AIAA Heterogenous Combustion Conference, Palm Beach, Florida, December 1963